Baseline Heavy Flavor Production at the LHC

R. Vogt

Nuclear Science Division, Lawrence Berkeley National Laboratory, Berkeley, CA 94720, USA

Physics Department, University of California, Davis, CA 95616, USA

Outline

- Theory of Heavy Flavor Production
- Total Cross Sections and Distributions
- Electrons from Heavy Flavor Decays

Charm as a Probe of Heavy Ion Collisions

Hard probe produced in the initial nucleon-nucleon collisions

Interacts strongly so its momentum can be modified by collisions during the evolution of the system leading to effects such as

- Energy loss in dense matter (Djordjevic et al, Lin et al, Kharzeev and Dokshitzer)
- Transverse momentum broadening due to hadronization from quark-gluon plasma (Svetitsky) or cold nuclear matter
- Collective flow of charm quarks (Lin and Molnar, Rapp et al)

In addition, if multiple $c\overline{c}$ pairs are produced in a given event, can enhance J/ψ (hidden charm) production (Thews et al)

pp and d+Au collisions serve as an important baseline for understanding medium effects on charm production, need good theoretical background and up-to-date open charm data

Charm Hadrons

Open charm hadron production and decay can be detected both through lepton channels (semi-leptonic decays) and through pure hadronic channels (reconstruction of the D mass, momentum)
Table shows that measuring D mesons alone is not enough to get total $c\overline{c}$ cross section

C	Mass (GeV)	$c\tau$ (μm)	$B(C \to lX)$ (%)	$B(C \to$ Hadrons) (%)
$D^+(c\overline{d})$	1.869	315	17.2	$K^-\pi^+\pi^+$ (9.1)
$D^-(\overline{c}d)$	1.869	315	17.2	$K^+\pi^-\pi^-$ (9.1)
$D^0(c\overline{u})$	1.864	123.4	6.87	$K^-\pi^+$ (3.8)
$\overline{D^0}(\overline{c}u)$	1.864	123.4	6.87	$K^+\pi^-$ (3.8)
$D^{*\pm}$	2.010			$D^0\pi^\pm$ (67.7), $D^\pm\pi^0$ (30.7)
D^{*0}	2.007			$D^0\pi^0$ (61.9)
$D_s^+(c\overline{s})$	1.969	147	8	$K^+K^-\pi^+$ (4.4), $\pi^+\pi^+\pi^-$ (1.01)
$D_s^-(\overline{c}s)$	1.969	147	8	$K^+K^-\pi^-$ (4.4), $\pi^+\pi^-\pi^-$ (1.01)
$\Lambda_c^+(udc)$	2.285	59.9	4.5	ΛX (35), $pK^-\pi^+$ (2.8)
$\Sigma_c^{++}(uuc)$	2.452			$\Lambda_c^+\pi^+$ (100)
$\Sigma_c^+(udc)$	2.451			$\Lambda_c^+\pi^0$ (100)
$\Sigma_c^0(ddc)$	2.452			$\Lambda_c^+\pi^-$ (100)
$\Xi_c^+(usc)$	2.466	132		$\Sigma^+K^-\pi^+$ (1.18)
$\Xi_c^0(dsc)$	2.472	29		$\Xi^-\pi^+$ (seen)

Table 1: Ground state charm hadrons with their mass, decay length (when given) and branching ratios to leptons (when applicable) and some prominent decays to hadrons, preferably to only charged hadrons although such decays are not always available.

Bottom Hadrons

Open bottom production and decay can also be detected both through lepton channels (semi-leptonic decays) and through pure hadronic channels (reconstruction of the B mass, momentum)

J/ψ decay channel is often used to obtain B cross section since J/ψ is "easy" to detect

Hadronic branching ratios small, two body decays to charged hadrons rare

B decays contribute to lepton spectra in two ways: direct $B \to lX$ and the indirect chain decay $B \to DX \to lX'$

Not much information available on bottom baryons

C	Mass (GeV)	$c\tau$ (μm)	$B(C \to lX)$ (%)	$B(C \to$ Hadrons) (%)
$B^+(u\overline{b})$	5.2790	501	10.2	$\overline{D}^0\pi^-\pi^+\pi^+$ (1.1), $J/\psi K^+$ (0.1)
$B^-(\overline{u}b)$	5.2790	501	10.2	$D^0\pi^+\pi^-\pi^-$ (1.1), $J/\psi K^-$ (0.1)
$B^0(d\overline{b})$	5.2794	460	10.5	$D^-\pi^+$ (0.276), $J/\psi K^+\pi^-$ (0.0325)
$\overline{B^0}(\overline{d}b)$	5.2794	460	10.5	$D^+\pi^-$ (0.276), $J/\psi K^-\pi^+$ (0.0325)
B_s^0	5.3696	438		$D_s^-\pi^+$ (< 13)
$B_c^+(c\overline{b})$	6.4			$J/\psi\pi^+$ (0.0082)
$B_c^-(\overline{c}b)$	6.4			$J/\psi\pi^-$ (0.0082)
$\Lambda_b^0(udb)$	5.624	368		$J/\psi\Lambda$ (0.047), $\Lambda_c^+\pi^-$ (seen)

Table 2: Known ground state bottom hadrons with their mass, decay length (when given), branching ratios to leptons (when applicable) and some selected decays to hadrons.

Calculating Heavy Flavors in Perturbative QCD

'Hard' processes have a large scale in the calculation that makes perturbative QCD applicable: high momentum transfer, μ^2, high mass, m, high transverse momentum, p_T, since $m \neq 0$, heavy quark production is a 'hard' process

Asymptotic freedom assumed to calculate the interactions between two hadrons on the quark/gluon level but the confinement scale determines the probability of finding the interacting parton in the initial hadron

Factorization assumed between the perturbative hard part and the universal, nonperturbative parton distribution functions

The hadronic cross section in an AB collision where $AB = pp, pA$ or nucleus-nucleus is

$$\sigma_{AB}(S, m^2) = \sum_{i,j=q,\overline{q},g} \int_{4m_Q^2/s}^1 \frac{d\tau}{\tau} \int dx_1\, dx_2\, \delta(x_1 x_2 - \tau) \times f_i^A(x_1, \mu_F^2)\, f_j^B(x_2, \mu_F^2)\, \widehat{\sigma}_{ij}(s, m^2, \mu_F^2, \mu_R^2)$$

f_i^A are the nonperturbative parton distributions, determined from fits to data, x_1 and x_2 are the fractional momentum of hadrons A and B carried by partons i and j, $\tau = s/S$

$\widehat{\sigma}_{ij}(s, m^2, \mu_F^2, \mu_R^2)$ is hard partonic cross section calculable in QCD in powers of α_s^{2+n}: leading order (LO), $n = 0$; next-to-leading order (NLO), $n = 1$ ...

Results depend strongly on quark mass, m, factorization scale, μ_F, in the parton densities and renormalization scale, μ_R, in α_s

Calculating the Total Cross Sections

Partonic total cross section only depends on quark mass m, not kinematic quantities

To NLO

$$\begin{aligned}\widehat{\sigma}_{ij}(s, m, \mu_F^2, \mu_R^2) &= \frac{\alpha_s^2(\mu_R^2)}{m^2}\left\{f_{ij}^{(0,0)}(\rho)\right. \\ &+ \left. 4\pi\alpha_s(\mu_R^2)\left[f_{ij}^{(1,0)}(\rho) + f_{ij}^{(1,1)}(\rho)\ln(\mu_F^2/m^2)\right] + \mathcal{O}(\alpha_s^2)\right\}\end{aligned}$$

$\rho = 4m^2/s$, s is partonic center of mass energy squared

μ_F is factorization scale, separates hard part from nonperturbative part

μ_R is renormalization scale, scale at which strong coupling constant α_s is evaluated

$\mu_F = \mu_R$ in evaluations of parton densities

$f_{ij}^{(a,b)}$ are dimensionless, μ-independent scaling functions, $a = 0$, $b = 0$ and $ij = q\overline{q}$, gg for LO, $a = 1$, $b = 0, 1$ and $ij = q\overline{q}$, gg and qg, $\overline{q}g$ for NLO

$f_{ij}^{(0,0)}$ are always positive, $f_{ij}^{(1,b)}$ can be negative also

Note that if $\mu_F^2 = m^2$, $f_{ij}^{(1,1)}$ does not contribute

Scaling Functions to NLO

Near threshold, $\sqrt{s}/2m \to 1$, Born contribution is large but dies away for $\sqrt{s}/2m \to \infty$

At large $\sqrt{s}/2m$, gg channel is dominant, then qg

High energy behavior of the cross sections due to phase space and low x behavior of parton densities

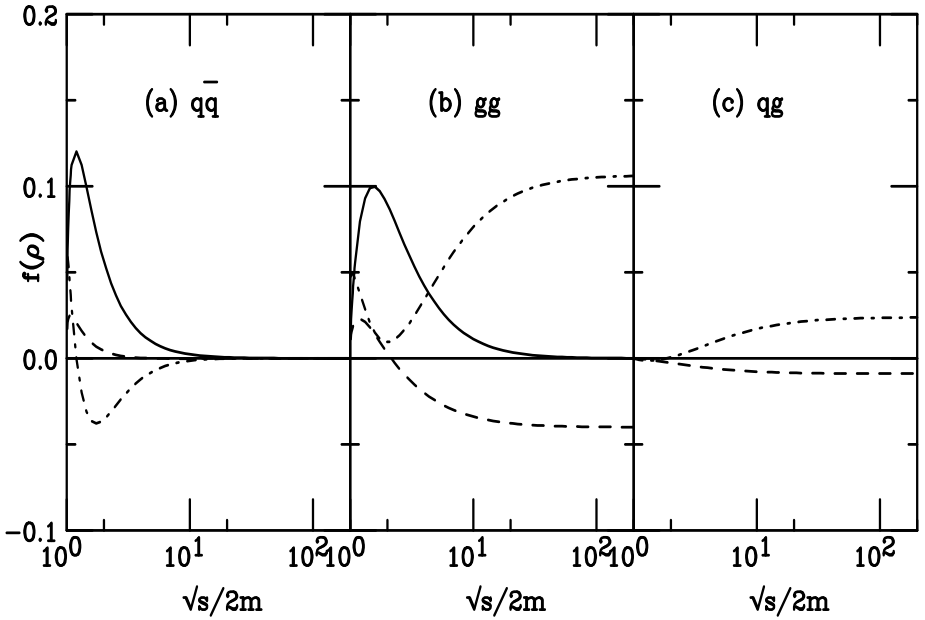

Figure 1: Scaling functions needed to calculate the total partonic $Q\overline{Q}$ cross section. The solid curves are the Born results, $f_{ij}^{(0,0)}$, the dashed and dot-dashed curves are NLO contributions, $f_{ij}^{(1,1)}$ and $f_{ij}^{(1,0)}$ respectively.

Comparison of $c\bar{c}$ Calculations to Data

Two ways to evaluate total cross sections and make predictions for higher energies

There are only 2 important parameters at fixed target energies: the quark mass m and the scale μ – at higher energies, the low x, low μ behavior of the parton densities plays an important role in the asymptotic result

The scale is usually chosen so that $\mu_F = \mu_R$, as in parton density fits although there is no strict reason for doing so for heavy flavors

First way (RV, Hard Probes Collaboration): fix m and $\mu \equiv \mu_F = \mu_R \geq m$ to data at lower energies and extrapolate to unknown regions – tends to favor lower masses

Second way (Cacciari, Nason and RV): determine an uncertainty band within $1.3 < m < 1.7$ GeV for charm and $4.5 < m < 5$ GeV for bottom with $(\mu_F/m, \mu_R/m) = (1,1)$, (2,2), (0.5,0.5), (0.5,1), (1,0.5), (1,2), (2,1)

We have to be careful with the resulting total charm cross sections for $\mu_F \leq m$ with the CTEQ6M parton densities since the minimum μ is 1.3 GeV, giving us big K factors for the lower scales and making the use of $\mu_F \leq m$ problematic, to say the least!

Densities like GRV98 have a lower starting scale, making their behavior for low x, low μ charm production less problematic

Note also that even the two-loop evaluation of α_s is big for low scales, for $m = 1.5$ GeV:
$\alpha_s(m/2 = 0.75) = 0.648$, $\alpha_s(m = 1.5) = 0.348$ and $\alpha_s(2m = 3) = 0.246$

CTEQ6M Densities at $\mu = m/2$, m and $2m$

CTEQ6M densities extrapolate to $\mu < \mu_{\min} = 1.3$ GeV

When backwards extrapolation leads to $xg(x,\mu) < 0$, then $xg(x,\mu) \equiv 0$

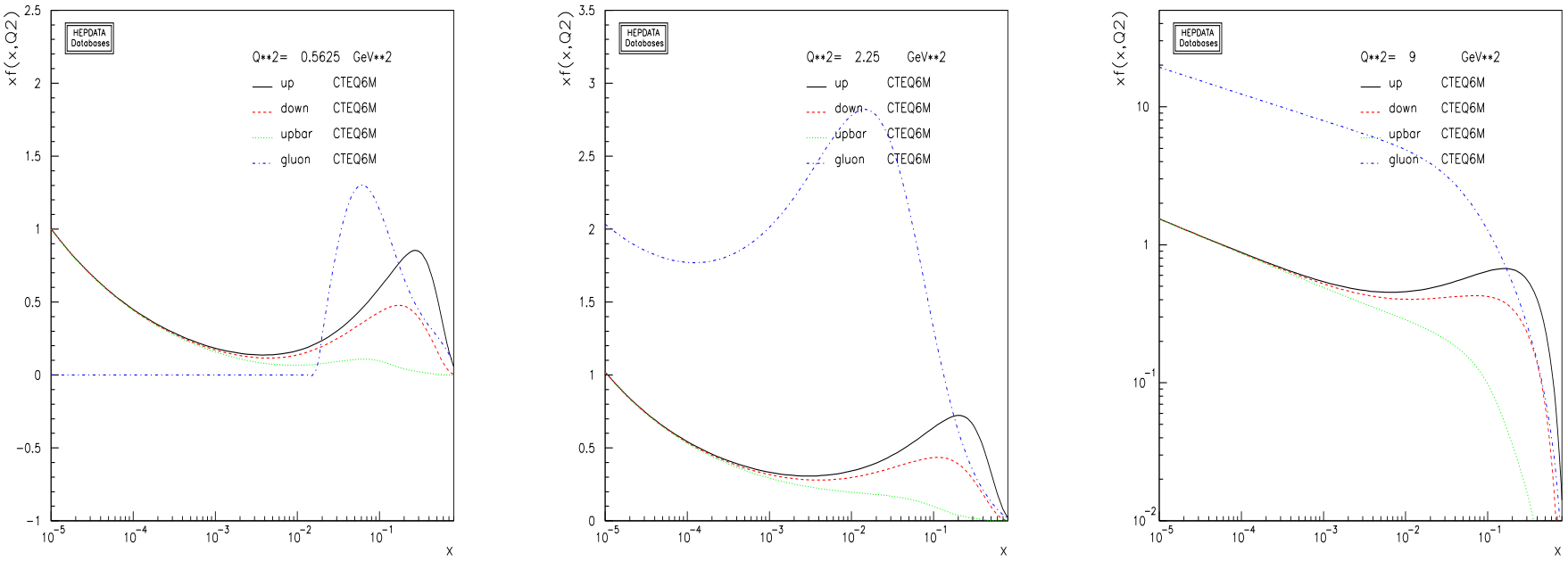

Figure 2: The CTEQ6M parton densities as a function of x for $\mu = m/2$ (left), $\mu = m$ (middle) and $\mu = 2m$ (right) for $m = 1.5$ GeV.

Fixing m and μ^2 to All Data: Method 1

Difficult to obtain a large calculated $c\overline{c}$ cross section with $\mu_F^2 = \mu_R^2$, as in parton density fits

Data favors lower masses – lowest mass used here is 1.2 GeV but much lower masses than allowed in pQCD needed to agree with largest cross sections

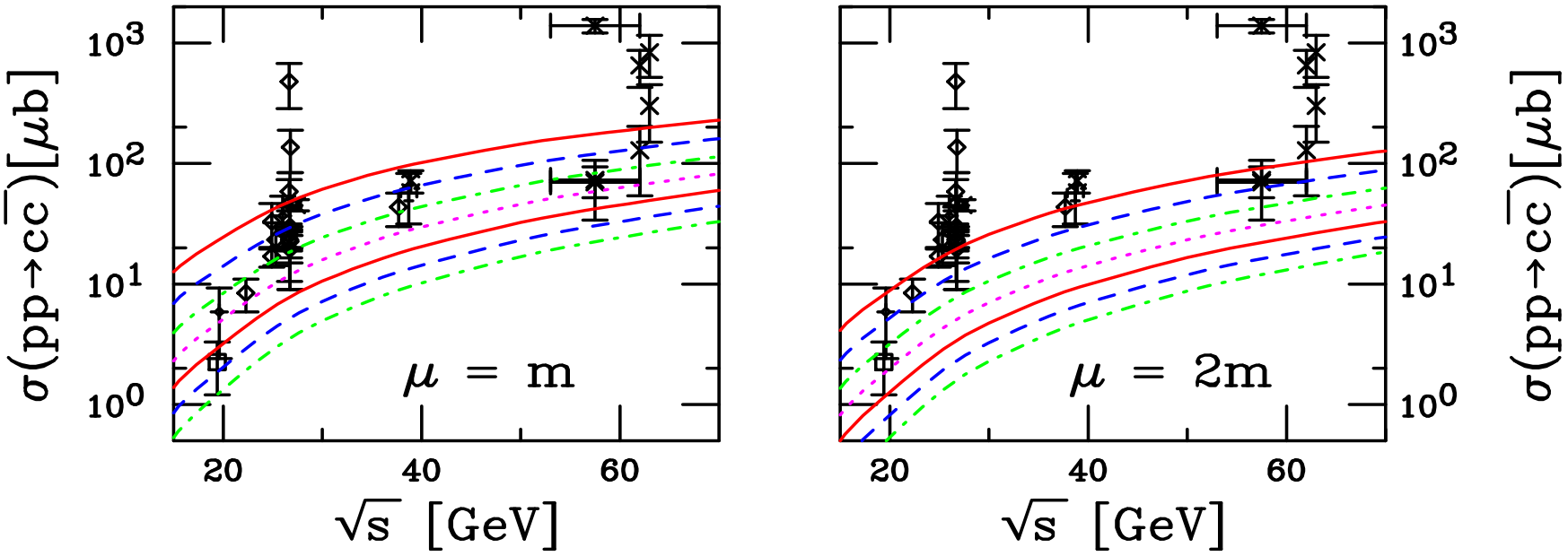

Figure 3: Total $c\overline{c}$ cross sections in pp and pA interactions up to ISR energies as a function of the charm quark mass using the CTEQ6M parton densities. The left-hand plot shows the results with $\mu_F = \mu_R = m$ while in the right-hand plot $\mu_F = \mu_R = 2m$. From top to bottom the curves are $m = 1.2$ (red), 1.3 (blue), 1.4 (green), 1.5 (magenta), 1.6 (red), 1.7 (blue), and 1.8 (green) GeV.

Extrapolation to Higher Energies

We have kept only the most recent measurements, including the PHENIX $\sqrt{S} = 130$ GeV result from Au+Au, lowest $\sqrt{S} = 200$ GeV point is from PHENIX pp

Note the $\mu = m$ behavior at high energy: the cross section grows slower with $\sqrt{s}$ due to the small x behavior of $xg(x, \mu)$ for μ close to $\mu_{\min}$

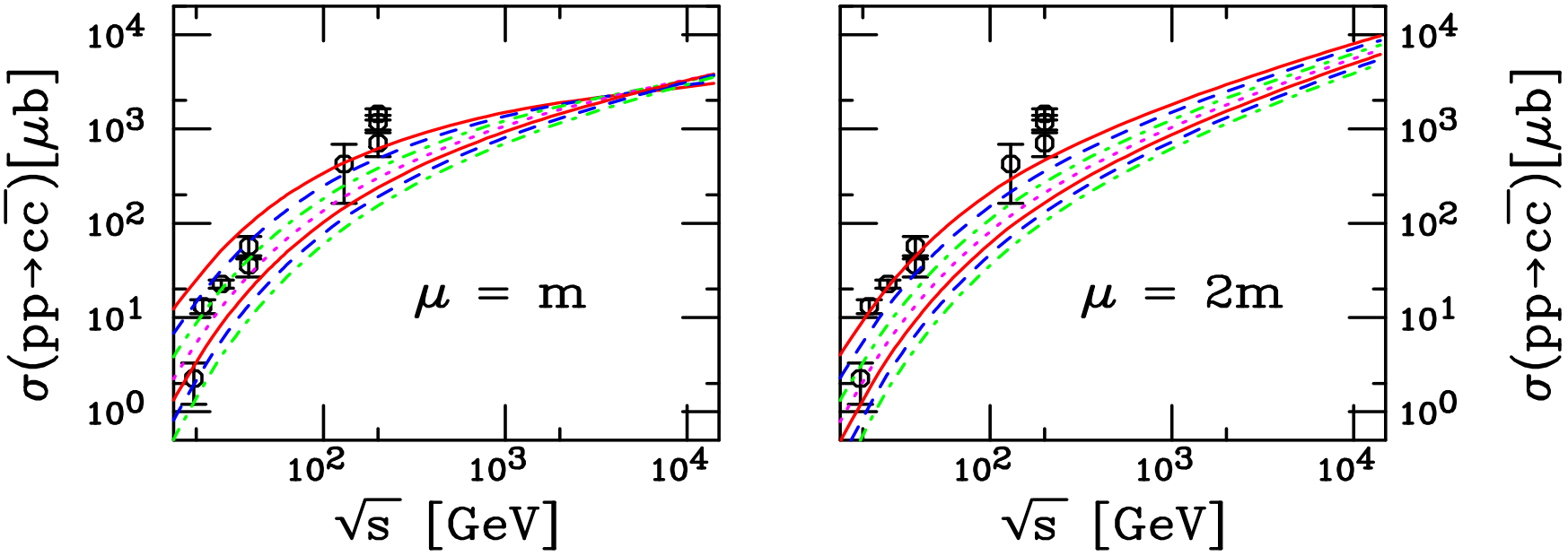

Figure 4: Same as previous but the energy range extended to LHC energies.

K Factors Using Method 1

K factors defined here as the ratio of the NLO to LO cross sections, both calculated with NLO parton densities and two loop evaluation of α_s

Note the $\mu = m$ behavior at high energy – K factors grow at low mass and then turn over due to both the low x parton densities and the fact that the LO cross section gets small far from threshold

The larger the value of μ, the better behaved the K factors

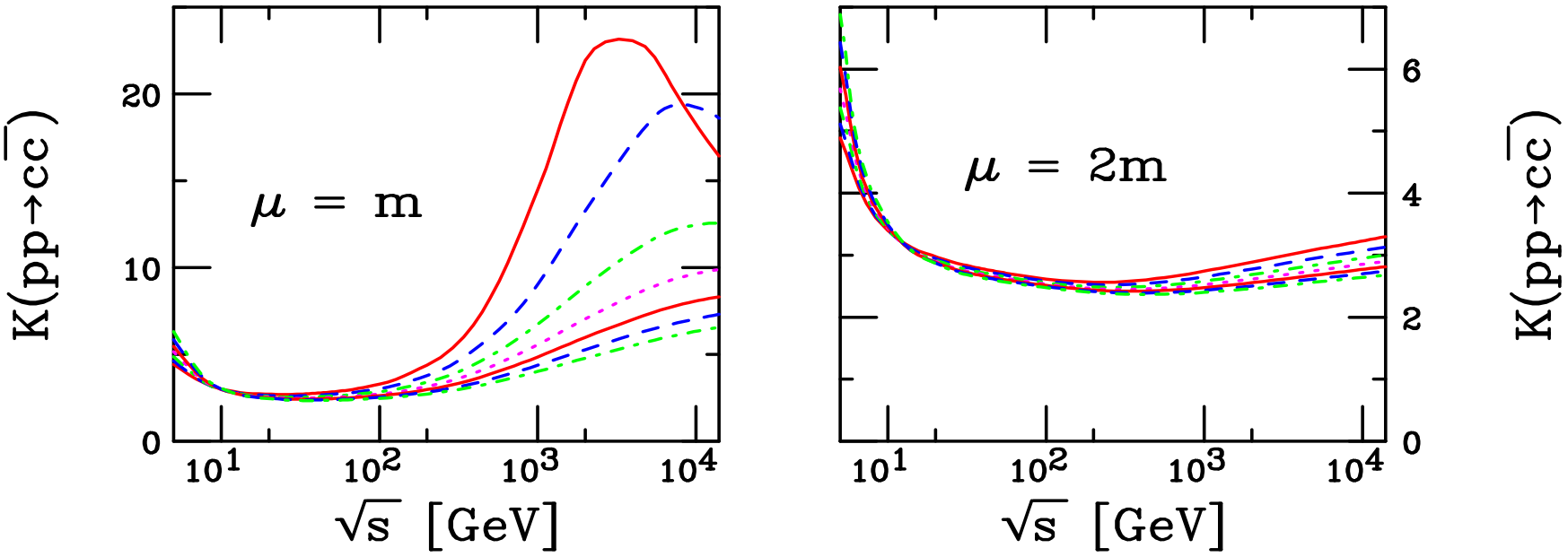

Figure 5: The K factors over the full $\sqrt{s}$ range, labeled as previously.

Theoretical Uncertainty Band: Method 2

Curves with $\mu_F \leq m$ flatten for $\sqrt{s} > 100$ GeV due to low x, low μ behavior of CTEQ6M – could be different for other PDF sets like GRV98

$(\mu_F/m, \mu_R/m) = (1, 0.5)$ and (0.5,0.5) have large total cross sections at RHIC since α_s big

Evolution faster at small x and high μ [(2,2), (2,1)]

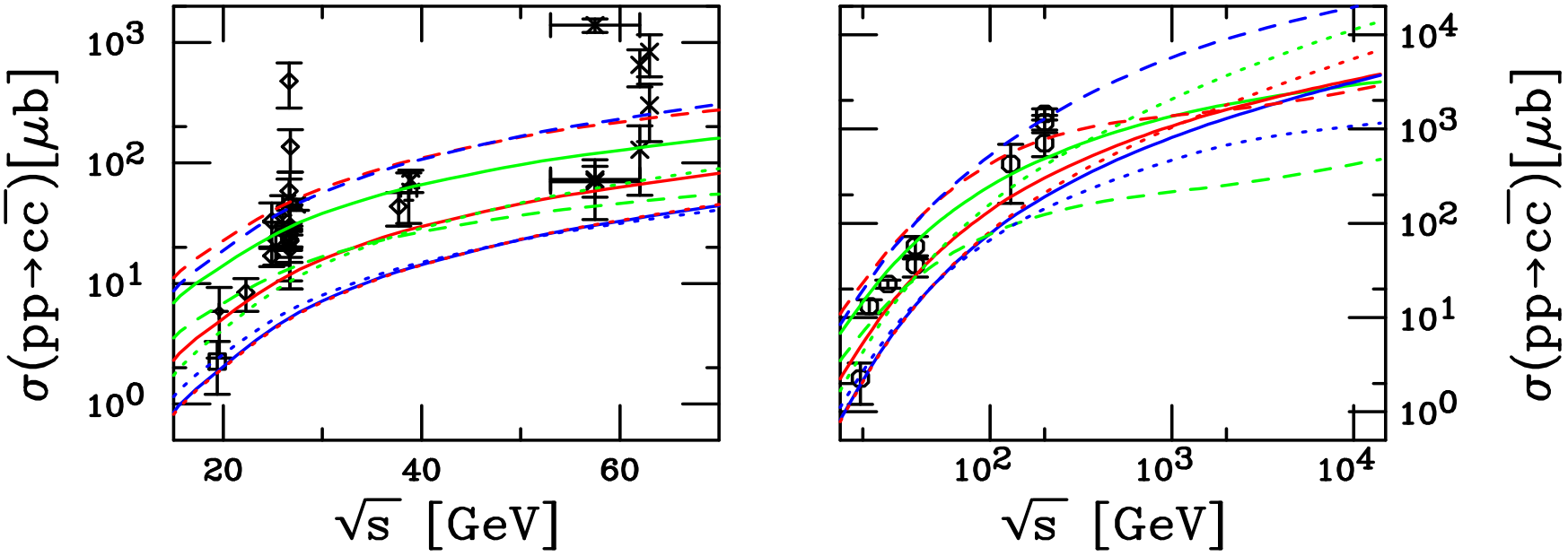

Figure 6: Total $c\bar{c}$ cross sections calculated using CTEQ6M. The solid red curve is the central value $(\mu_F/m, \mu_R/m) = (1, 1)$ with $m = 1.5$ GeV. The green and blue solid curves are $m = 1.3$ and 1.7 GeV with (1,1) respectively. The red, blue and green dashed curves correspond to (0.5,0.5), (0.5,1) and (1,0.5) respectively while the red, blue and green dotted curves are for (2,2), (2,1) and (1,2) respectively, all for $m = 1.5$ GeV.

Theoretical Uncertainty Band: K Factors

Results with $(\mu_F/m, \mu_R/m) = (1, 0.5)$ and (0.5,0.5) have largest K factors

Results with (1,1), (2,2), (2,1) and (1,2) with $m = 1.5$ GeV and (1,1) with $m = 1.7$ GeV give $K < 10$ at highest energies

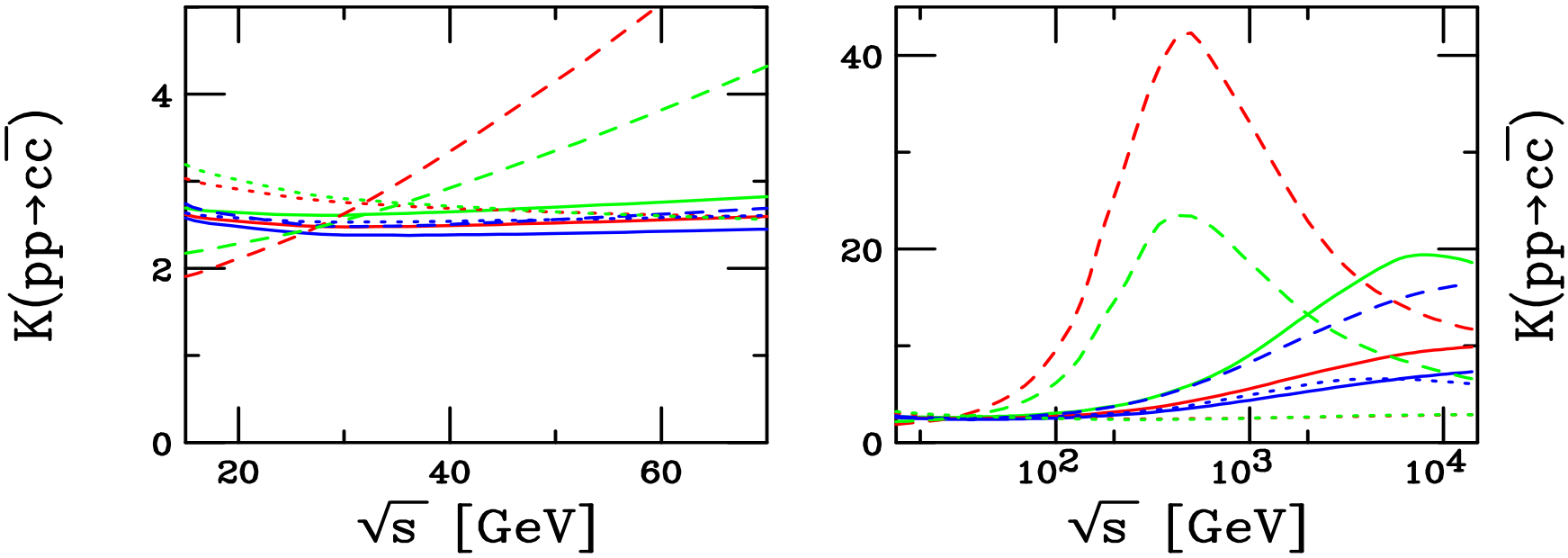

Figure 7: The $c\bar{c}$ K factors calculated using CTEQ6M. The solid red curve is the central value $(\mu_F/m, \mu_R/m) = (1, 1)$ with $m = 1.5$ GeV. The green and blue solid curves are $m = 1.3$ and 1.7 GeV with (1,1) respectively. The red, blue and green dashed curves correspond to (0.5,0.5), (1,0.5) and (0.5,1) respectively while the red, blue and green dotted curves are for (2,2), (1,2) and (2,1) respectively, all for $m = 1.5$ GeV.

Comparison of Bottom Calculations to Data

Fewer data on bottom production in pp collisions, especially on total cross section

Bottom production is less problematic because, even for $\mu = m/2$, we are well above $\mu_{\rm min}$ of parton densities, extrapolation to higher energies should also be better

Fixing m and μ^2 to All Data: Method 1

Latest HERA-B point not shown, lies below previous point

In this approach, $m = 5$ GeV, $\mu = m/2$; $m = 4.75$ GeV, $\mu = m$; and $m = 4.5$ GeV, $\mu = 2m$ are all close to center of data .

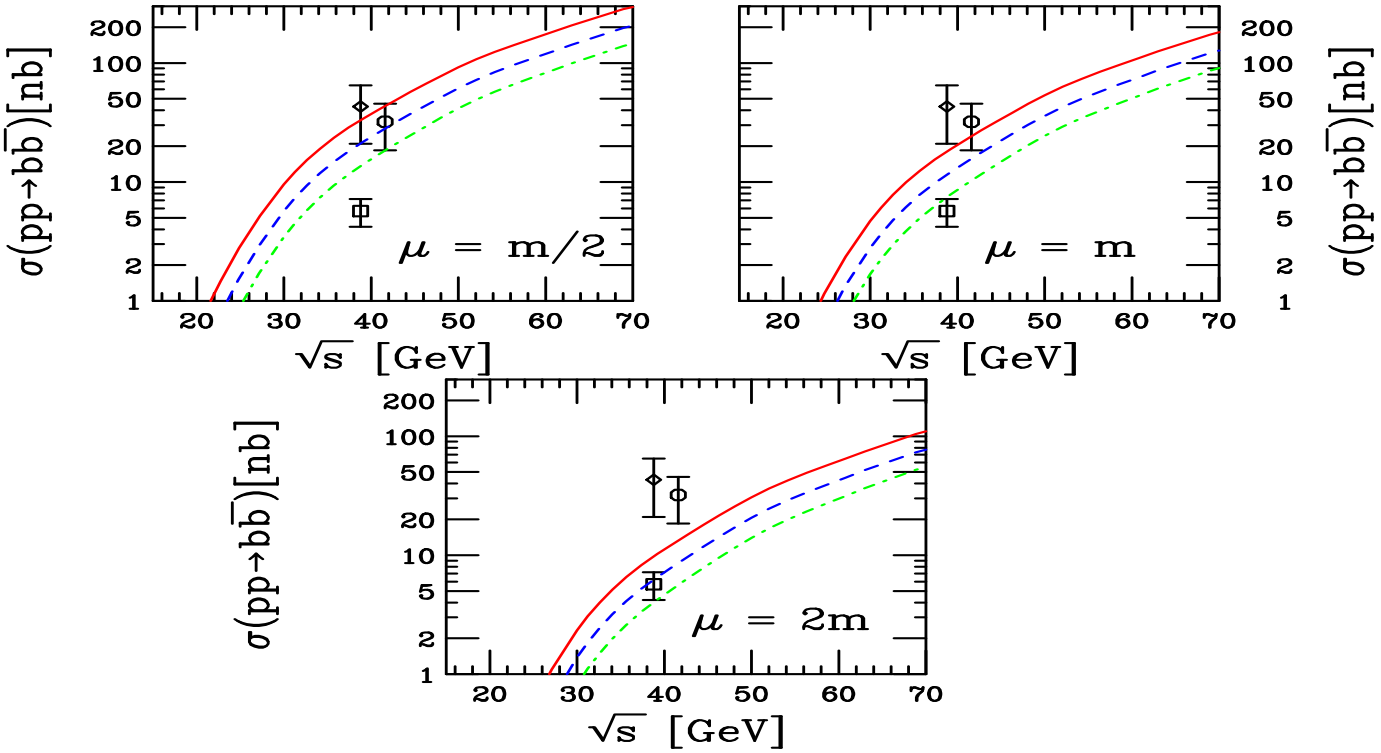

Figure 8: Total $b\bar{b}$ cross sections in pp and pA interactions as a function of the bottom quark mass using the CTEQ6M parton densities. Clockwise from upper left, the plots give results for $\mu = m/2$, $\mu = m$ and $\mu = 2m$. The mass values are 4.5 GeV (solid red), 4.75 GeV (dashed blue) and 5 GeV (dot-dashed green).

Extrapolation to Higher Energies

Asymptotic behavior very similar for bottom, no surprises

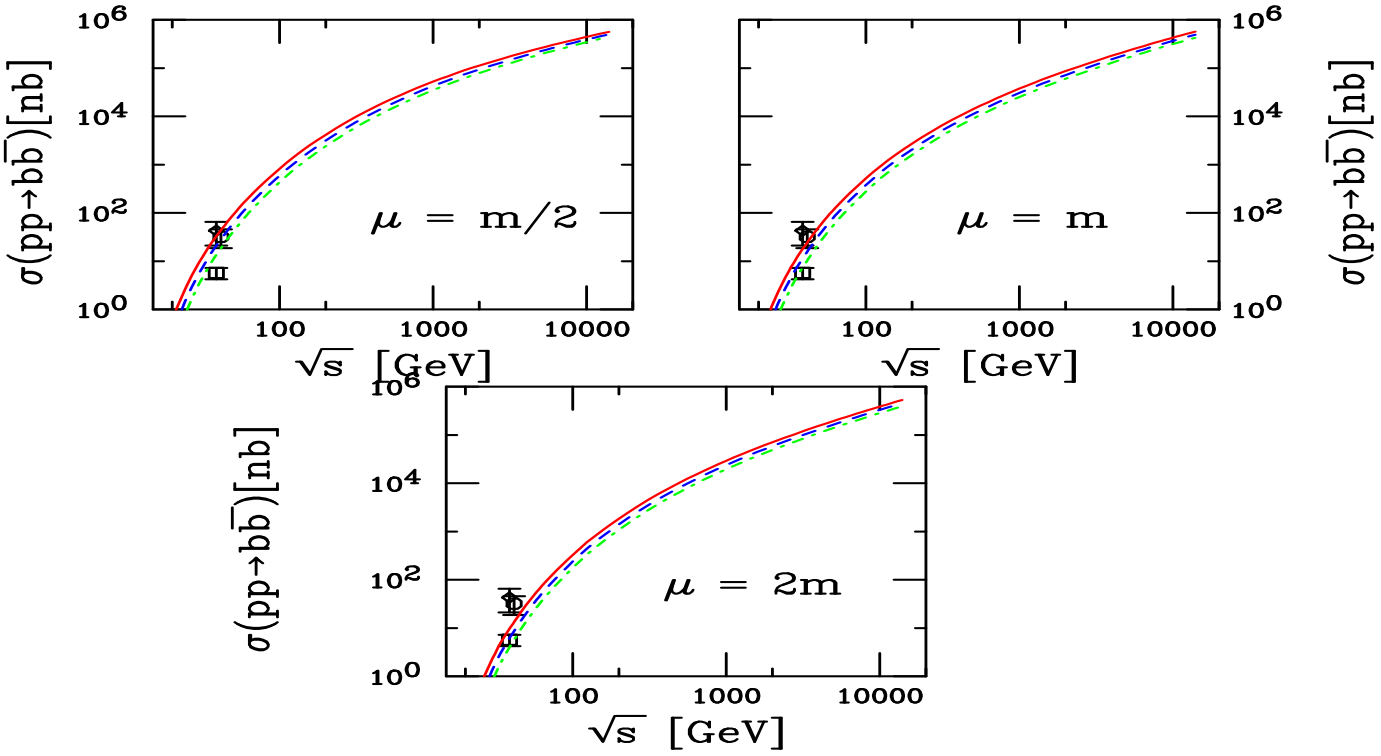

Figure 9: Same as previous but the energy range extended to LHC energies.

K Factors Using Method 1

K factors better behaved for bottom production, x and μ not so small as for charm, consequently α_s is smaller also

K factors much smaller at higher energy than charm, strong growth only seen for $\mu = m/2$, smallest K factors for $\mu = 2m$, also the case with charm

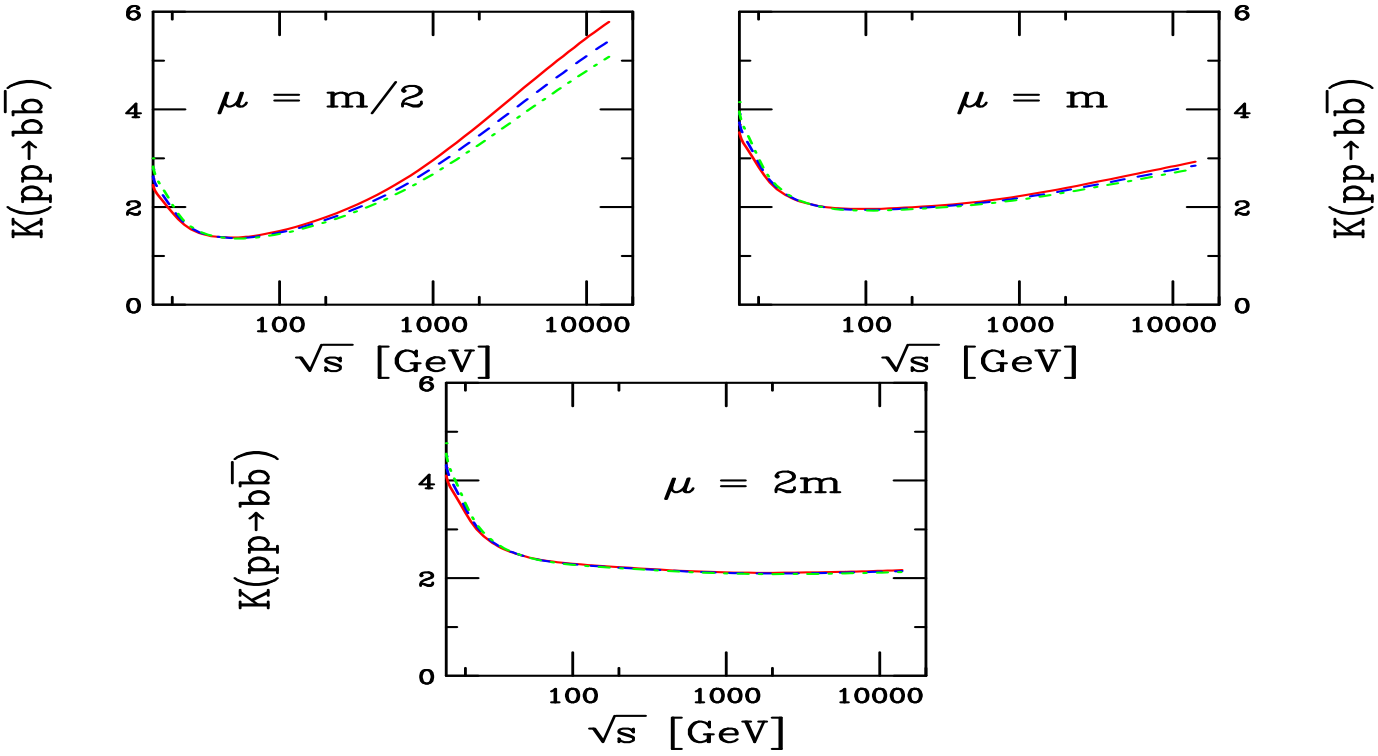

Figure 10: The K factors over the full $\sqrt{s}$ range, labeled as before.

Theoretical Uncertainty Band: Method 2

More sensible to talk about uncertainty band for bottom than for charm

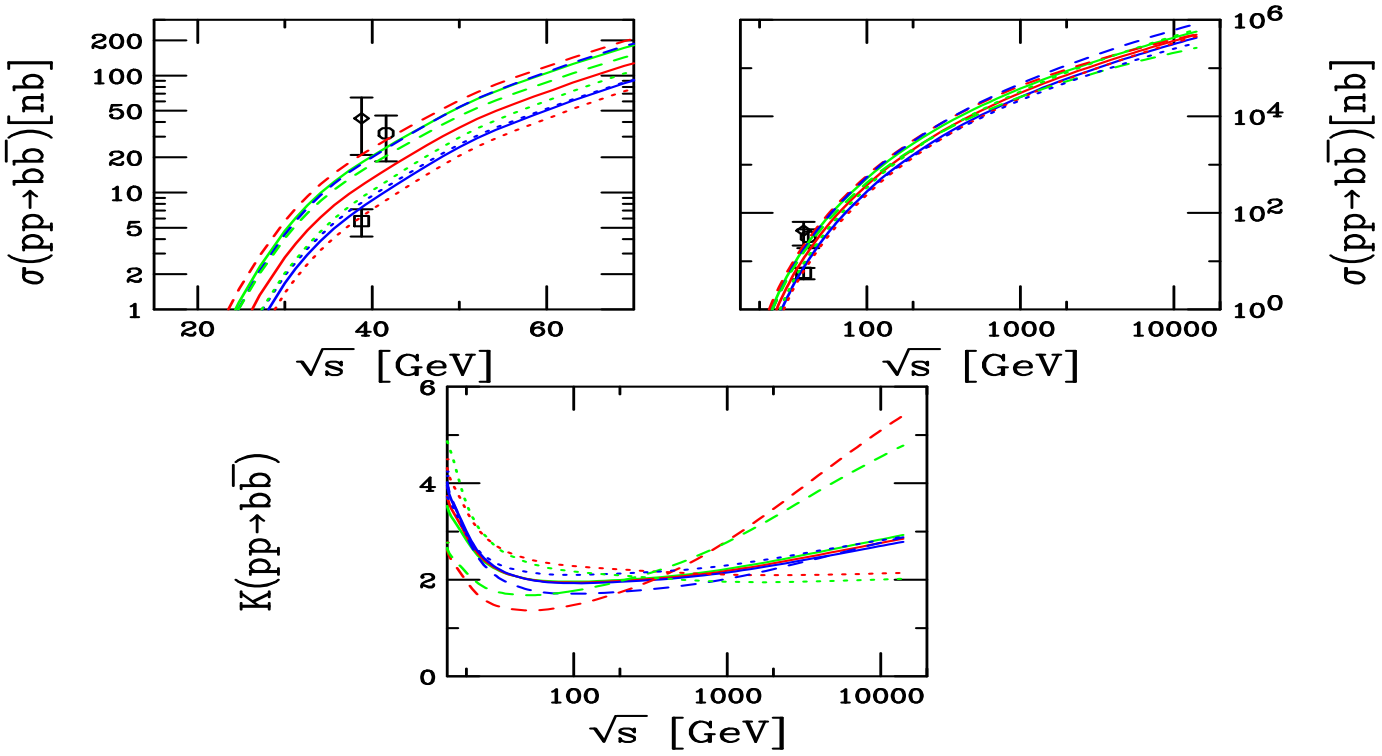

Figure 11: Total $b\bar{b}$ cross sections calculated using CTEQ6M. The solid red curve is the central value $(\mu_F/m, \mu_R/m) = (1, 1)$ with $m = 4.75$ GeV. The green and blue solid curves are $m = 4.5$ and 5 GeV with (1,1) respectively. The red, blue and green dashed curves correspond to (0.5,0.5), (1,0.5) and (0.5,1) respectively while the red, blue and green dotted curves are for (2,2), (1,2) and (2,1) respectively, all for $m = 4.75$ GeV.

From Total Cross Sections to Distributions

Distributions as a function of kinematic variables can provide more information than the total cross section

In total cross section, the quark mass is the only relevant scale

When considering kinematic observables like x_F or p_T, the momentum scale is also relevant so that, instead of $\mu^2 \propto m^2$, one usually uses $\mu^2 \propto m_T^2$ – this difference makes the p_T-integrated total cross section decrease a bit relative to that calculated using the dimensionless scaling functions

Fragmentation also important when discussing observables

Fragmentation universal, like parton densities, so the parameterizations of e^+e^- data should work in hadroproduction – new determinations of the charm to D fragmentation in Mellin space result in a softer, more accurate spectra than the old Peterson function

NLO Bare Quark p_T Distributions

Differences largest at low p_T, determines total cross section

Distributions become similar at high p_T

Average p_T increases with m and decreases with μ

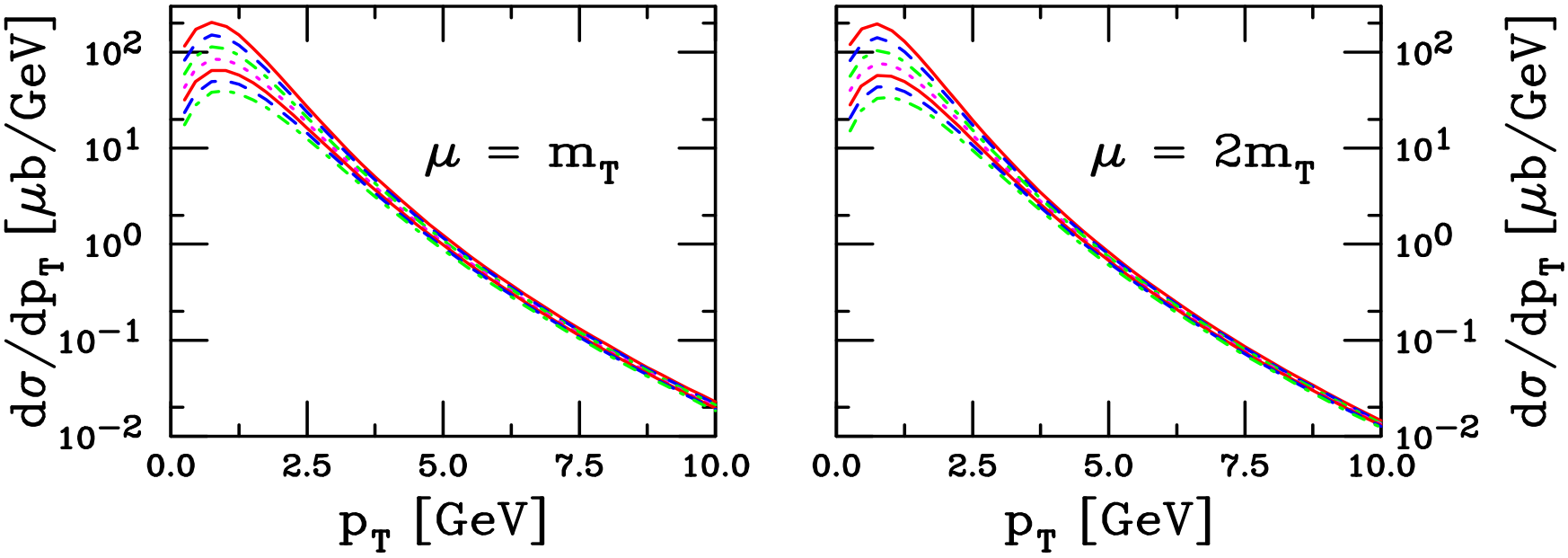

Figure 12: The NLO charm quark p_T distributions in pp interactions at $\sqrt{S} = 200$ GeV as a function of the charm quark mass calculated with the GRV98 HO parton densities, integrated over all rapidity. The left-hand plot shows the results with the renormalization and factorization scales equal to m_T while in the right-hand plot the scale is set to $2m_T$. From top to bottom the curves are $m = 1.2$ (red), 1.3 (blue), 1.4 (green), 1.5 (magenta), 1.6 (red), 1.7 (blue), and 1.8 (green) GeV.

Calculation of p_T Dependence

FONLL calculation designed to cure large logs of p_T/m for $p_T \gg m$ in fixed order calculation (FO) where mass is no longer only relevant scale

Includes resummed terms (RS) of order $\alpha_s^2(\alpha_s \log(p_T/m))^k$ (leading log – LL) and $\alpha_s^3(\alpha_s \log(p_T/m))^k$ (NLL) while subtracting off fixed order terms retaining only the logarithmic mass dependence (the "massless" limit of fixed order (FOM0)), both calculated in the same renormalization scheme

There needs to be a scheme change in the FO calculation since it treats the heavy flavor as heavy while the RS approach includes the heavy flavor as an active light degree of freedom

Schematically then:

$$\text{FONLL} = \text{FO} + (\text{RS} - \text{FOM0})G(m, p_T)$$

The function $G(m, p_T)$ is arbitrary but must approach unity as $m/p_T \to 0$ up to terms suppressed by powers of m/p_T

Problems arise with FONLL resummed part away from midrapidity above RHIC energies, LHC results shown for fixed order (NLO) only

Calculations here done using the FONLL code at fixed order to make tables from fragmentation and decay – could do FONLL for $|y| \leq 1$ but decays need broader y range

FONLL slopes should be steeper than NLO

Comparison of FONLL and NLO p_T Distributions

FONLL result for bare charm is slightly higher over most of the p_T range – fixed order result gets higher at large p_T due to large $\log(p_T/m)$ terms

New fragmentation functions (dashed) for D^0 harder than Peterson function (dot-dot-dot-dashed)

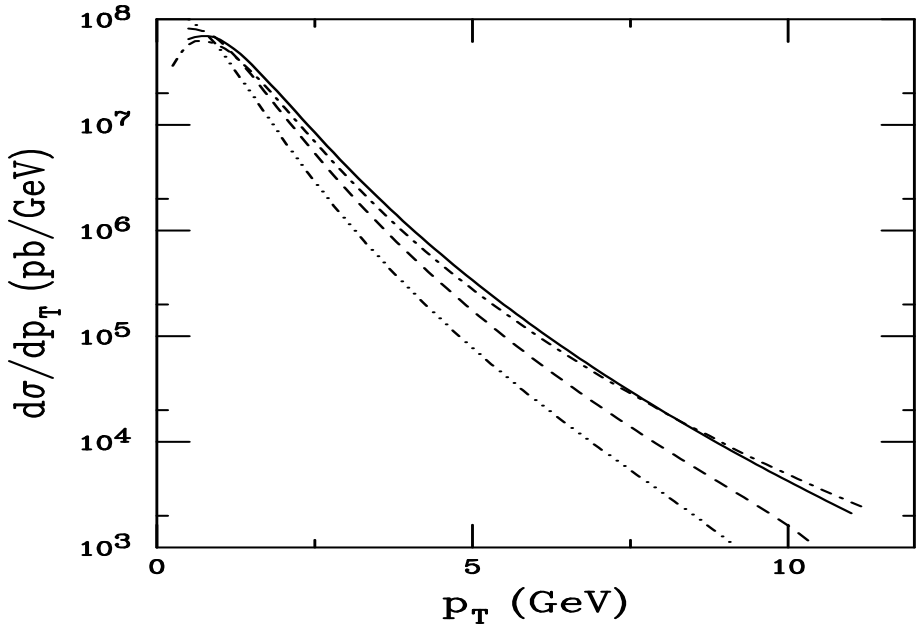

Figure 13: The p_T distributions calculated using FONLL are compared to NLO. The dot-dashed curve is the NLO charm quark p_T distribution. The solid, dashed and dot-dot-dot-dashed curves are FONLL results for the charm quark and D^0 meson with the updated fragmentation function and the Peterson function, respectively. All the calculations are done with the CTEQ6M parton densities, $m = 1.2$ GeV and $\mu = m_T$ in the region $|y| \leq 0.75$.

Uncertainty Bands for p_T Distributions

As we saw for the total cross sections, depending on μ_R, μ_F and m, the maximum and minimum values of the calculated total cross section may come from different curves

Same is true for p_T distributions: upper and lower curves in the band do not represent a single set of μ_R, μ_F and m values but are the upper and lower limits of mass and scale uncertainties added in quadrature:

$$(d\sigma/dp_T)_{\rm max} = (d\sigma/dp_T)_{\rm central} + \sqrt{((d\sigma/dp_T)_{\mu,\rm max} - (d\sigma/dp_T)_{\rm central})^2 + ((d\sigma/dp_T)_{m,\rm max} - (d\sigma/dp_T)_{\rm central})^2}$$
$$(d\sigma/dp_T)_{\rm min} = (d\sigma/dp_T)_{\rm central} - \sqrt{((d\sigma/dp_T)_{\mu,\rm min} - (d\sigma/dp_T)_{\rm central})^2 + ((d\sigma/dp_T)_{m,\rm min} - (d\sigma/dp_T)_{\rm central})^2}$$

The central value is $m = 1.5$ GeV, $\mu_F = \mu_R = m_T$

Previous results with $m = 1.2$ GeV, $\mu_F = \mu_R = 2m_T$ fall within the uncertainty band

We give results for bare heavy flavors, heavy flavor mesons and semileptonic decays in pp collisions at $\sqrt{s} = 5.5$ TeV and compare cross sections at 8.8 and 14 TeV

Note that, due to the scale change from m to m_T in the p_T distributions leads to much lower integrated total cross sections for $(\mu_F/m_T, \mu_R/m_T) = (1, 0.5)$ and (0.5,0.5) since $\alpha_s(m_T)$ decreases with p_T

Components of Uncertainty Band at 200 GeV

Curves with $(\mu_F/m_T, \mu_R/m_T) = (1, 0.5)$ and (0.5,0.5) make up the upper scale uncertainty while those with (0.5,1) and (2,2) make up the lower

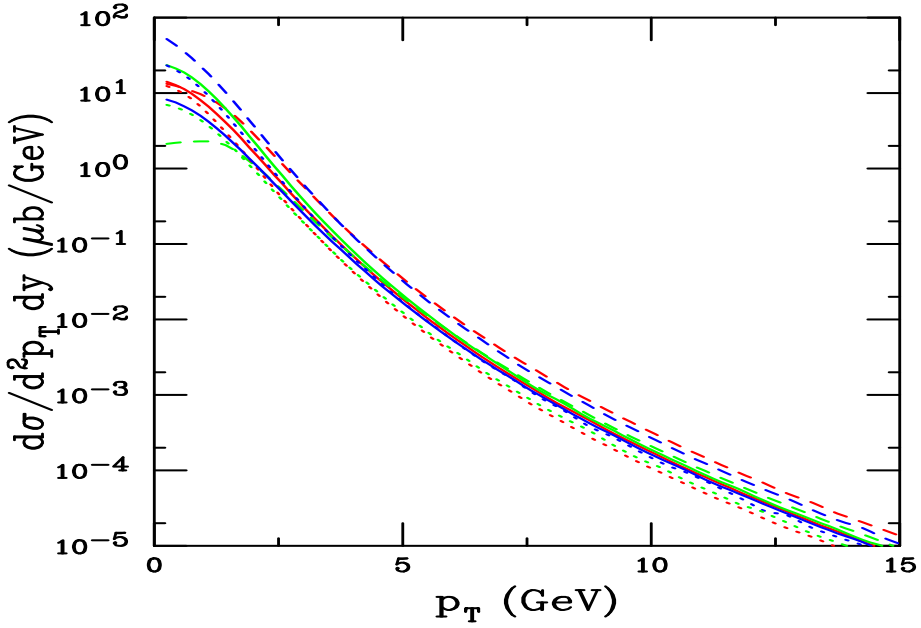

Figure 14: The charm quark p_T distributions calculated using CTEQ6M. The solid red curve is the central value $(\mu_F/m_T, \mu_R/m_T) = (1, 1)$ with $m = 1.5$ GeV. The green and blue solid curves are $m = 1.3$ and 1.7 GeV with (1,1) respectively. The red, blue and green dashed curves correspond to (0.5,0.5), (1,0.5) and (0.5,1) respectively while the red, blue and green dotted curves are for (2,2), (1,2) and (2,1) respectively, all for $m = 1.5$ GeV.

Uncertainty Bands for c and D at 200 GeV

NLO and FONLL bands almost indistinguishable from each other, slight difference in normalization between the two at forward rapidities due to limitations on FONLL at large rapidity

D meson band uses primary D distributions, not distinguishing charged from neutral D mesons, not possible to separate c and D bands for $p_T < 10$ GeV

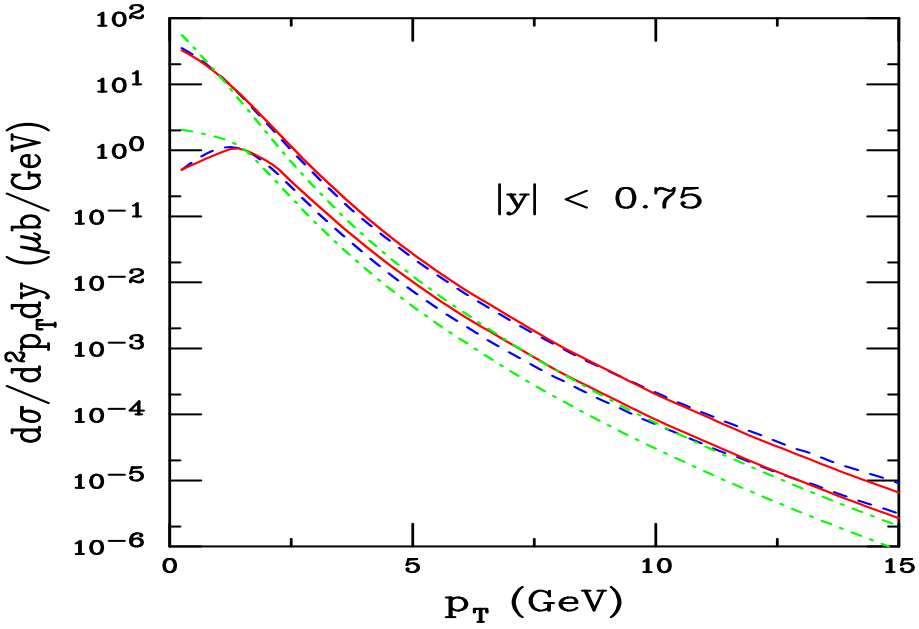

Figure 15: The charm quark theoretical uncertainty band as a function of p_T for FONLL (red solid curves) and NLO (blue dashed curves) in $\sqrt{s} = 200$ GeV pp collisions. Also shown is the D meson uncertainty band (green dot-dashed curves), all using the CTEQ6M parton densities for $|y| \leq 0.75$.

Components of Uncertainty Band at 5.5 TeV

NLO only here, true FONLL result should be steeper at low p_T

Sharp turnover for $(\mu_F/m_T, \mu_R/m_T) = (0.5, 0.5)$ and (1,0.5)

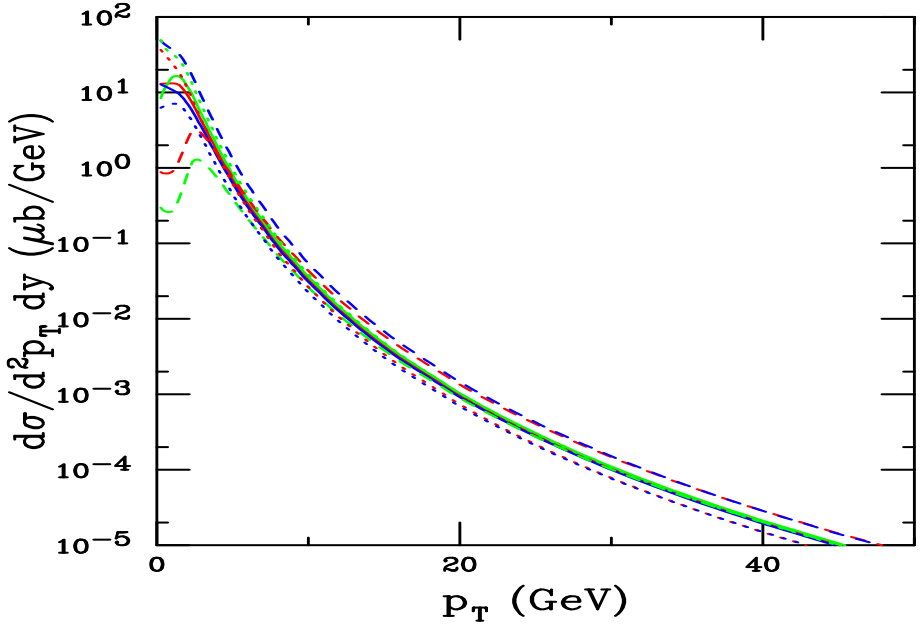

Figure 16: The charm quark p_T distributions calculated using CTEQ6M. The solid red curve is the central value $(\mu_F/m_T, \mu_R/m_T) = (1, 1)$ with $m = 1.5$ GeV. The green and blue solid curves are $m = 1.3$ and 1.7 GeV with (1,1) respectively. The red, blue and green dashed curves correspond to (0.5,0.5), (1,0.5) and (0.5,1) respectively while the red, blue and green dotted curves are for (2,2), (1,2) and (2,1) respectively, all for $m = 1.5$ GeV.

Uncertainty Bands for c and D at 5.5 TeV

c and D distributions are harder at 500 GeV

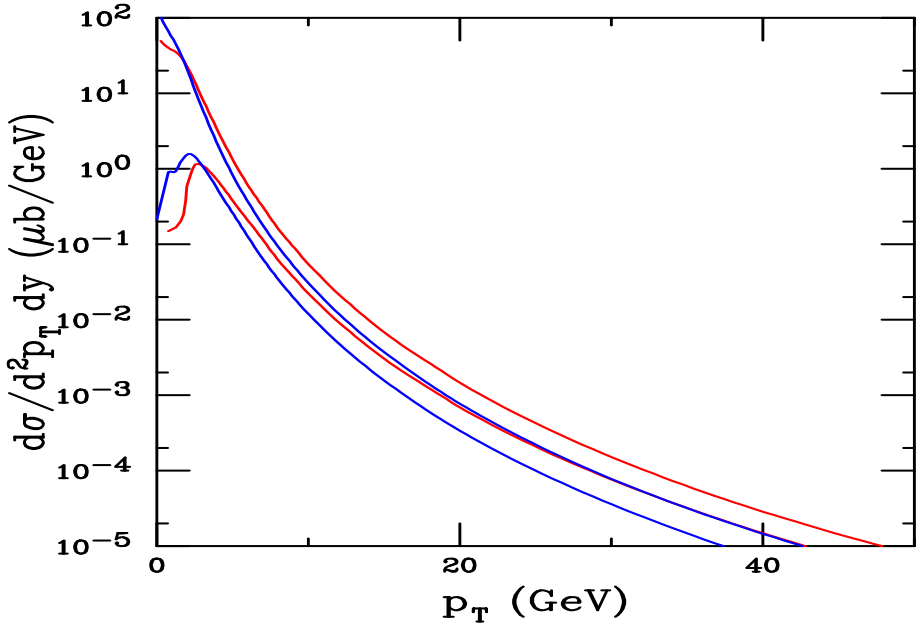

Figure 17: The charm quark theoretical uncertainty band as a function of p_T at NLO (red curves) in $\sqrt{s} = 5.5$ TeV pp collisions. Also shown is the D meson uncertainty band (blue curves), all using the CTEQ6M parton densities for $|y| \leq 1$.

Comparison of NLO Charm Rapidity Distributions

pp distributions broader at 5.5 TeV

Note that the importance of the various mass and scale choices differ considerably between the two energies: faster Q^2 evolution at small x with higher scales

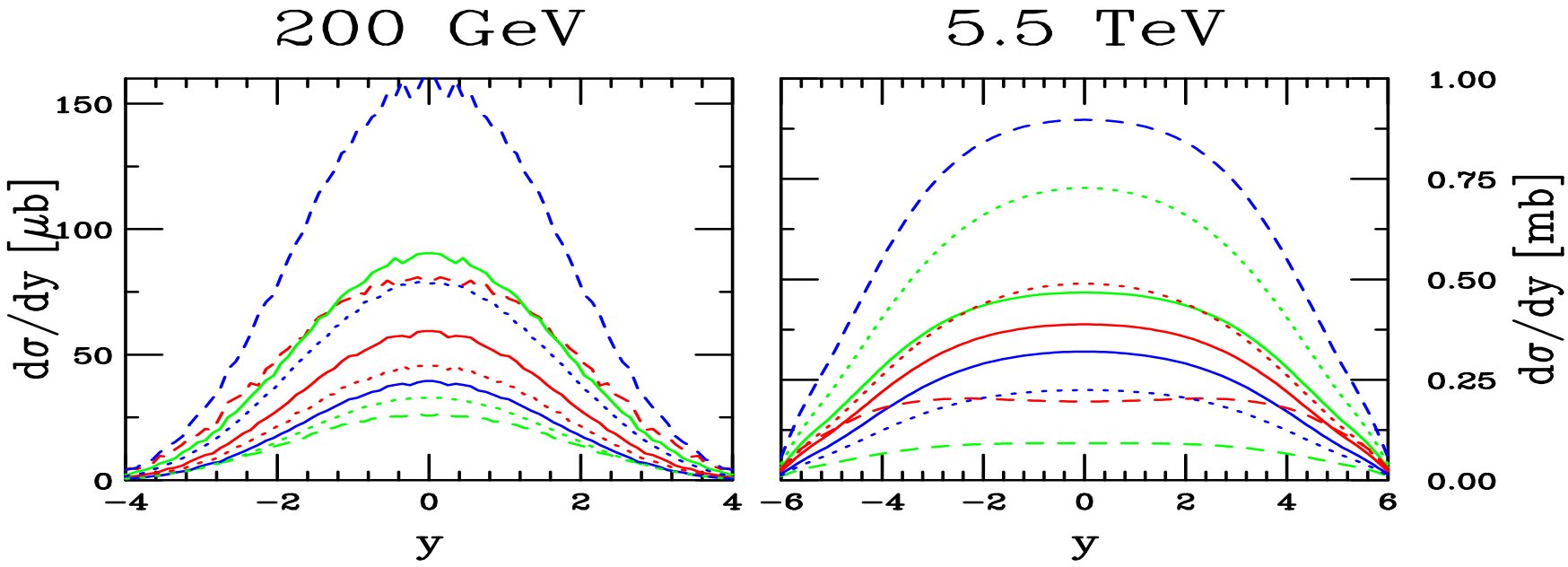

Figure 18: The charm quark rapidity distributions calculated using CTEQ6M in *pp* collisions at $\sqrt{s} = 200$ GeV (left-hand side) and 5.5 TeV (right-hand side). The solid red curve is the central value $(\mu_F/m_T, \mu_R/m_T) = (1, 1)$ with $m = 1.5$ GeV. The green and blue solid curves are $m = 1.3$ and 1.7 GeV with (1,1) respectively. The red, blue and green dashed curves correspond to (0.5,0.5), (1,0.5) and (0.5,1) respectively while the red, blue and green dotted curves are for (2,2), (1,2) and (2,1) respectively, all for $m = 1.5$ GeV.

Charm Cross Sections

m (GeV)	μ_F/m_T	μ_R/m_T	$\sigma(200\,\text{GeV})$ (mb)	$\sigma(5.5\,\text{TeV})$ (mb)	$\sigma(8.8\,\text{TeV})$ (mb)	$\sigma(14\,\text{TeV})$ (mb)
1.3	1	1	0.367	3.80	5.14	6.90
1.5	1	1	0.234	3.04	4.16	5.63
1.7	1	1	0.151	2.42	3.34	4.58
1.5	0.5	0.5	0.369	2.11	2.68	3.44
1.5	1	0.5	0.649	8.01	10.85	14.53
1.5	0.5	1	0.110	0.80	1.05	1.38
1.5	2	2	0.180	3.65	5.16	7.21
1.5	1	2	0.129	1.68	2.30	3.13
1.5	2	1	0.318	5.66	7.95	11.03

Table 3: Charm cross sections obtained from the parameter sets used to determined the theoretical uncertainty band in pp collisions with the CTEQ6M densities.

Uncertainty Bands for b and B at 200 GeV

Bands narrower for bottom than for charm and impossible to separate b from B over the p_T range shown (B is a generic B meson)

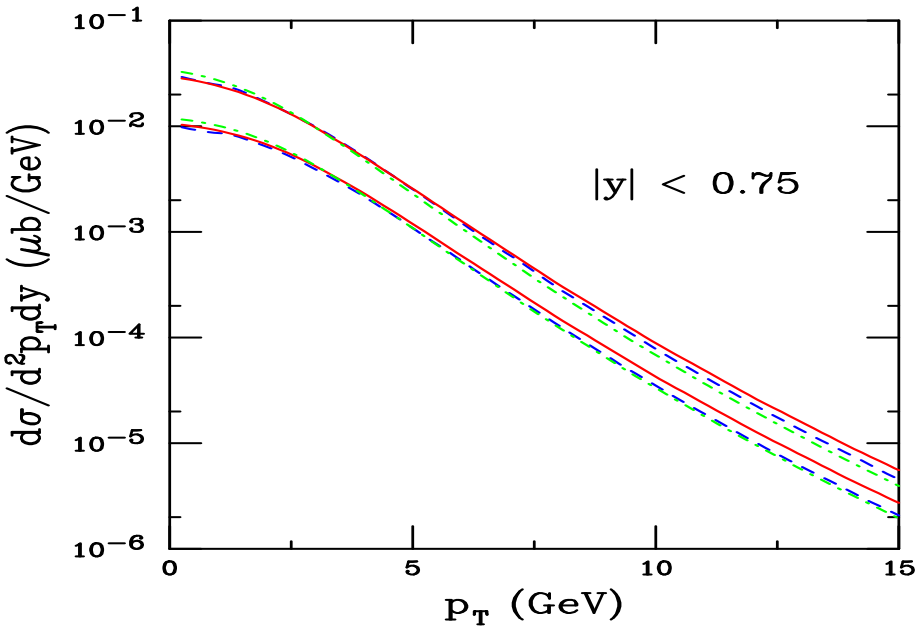

Figure 19: The bottom quark theoretical uncertainty band as a function of p_T for FONLL (red solid curves) and NLO (blue dashed curves) in $\sqrt{s} = 200$ GeV pp collisions. Also shown is the B meson uncertainty band (green dot-dashed curves), all using the CTEQ6M parton densities for $|y| \leq 0.75$.

Uncertainty Bands for b and B at 5.5 TeV

Much stronger energy dependence and more hardening for bottom than for charm with increasing energy .

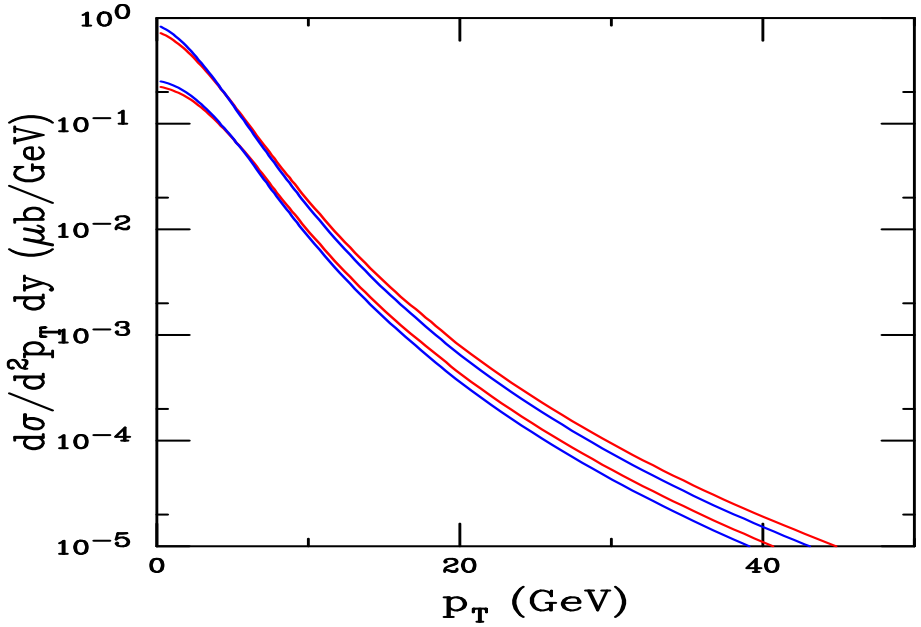

Figure 20: The bottom quark theoretical uncertainty band as a function of p_T at NLO (red curves) in $\sqrt{s} = 5.5$ TeV pp collisions. Also shown is the B meson uncertainty band (blue curves), all using the CTEQ6M parton densities for $|y| \leq 1$.

Comparison of NLO Bottom Rapidity Distributions

pp distributions broader at 5.5 TeV

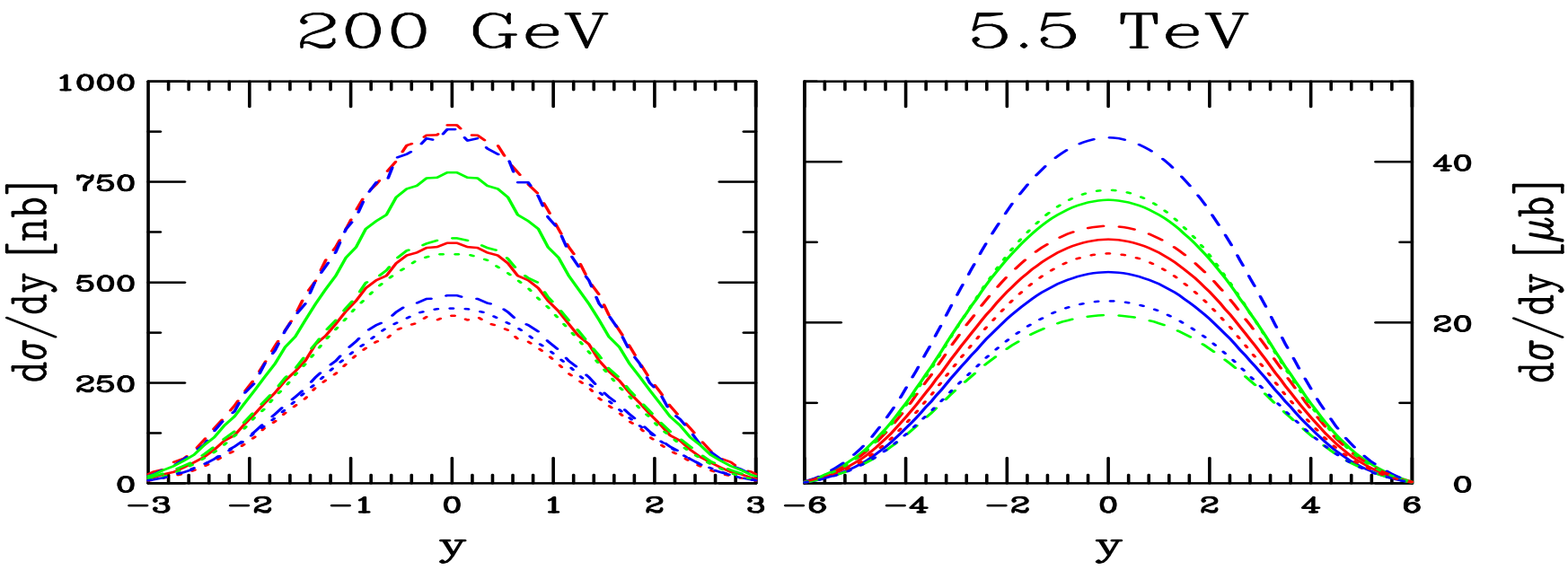

Figure 21: The bottom quark rapidity distributions calculated using CTEQ6M in *pp* collisions at $\sqrt{s} = 200$ GeV (left-hand side) and 5.5 TeV (right-hand side). The solid red curve is the central value $(\mu_F/m_T, \mu_R/m_T) = (1, 1)$ with $m = 4.75$ GeV. The green and blue solid curves are $m = 4.5$ and 5 GeV with (1,1) respectively. The red, blue and green dashed curves correspond to (0.5,0.5), (1,0.5) and (0.5,1) respectively while the red, blue and green dotted curves are for (2,2), (1,2) and (2,1) respectively, all for $m = 4.75$ GeV.

Bottom Cross Sections

m (GeV)	μ_F/m_T	μ_R/m_T	$\sigma(200\,\text{GeV})$ (μb)	$\sigma(5.5\,\text{TeV})$ (μb)	$\sigma(8.8\,\text{TeV})$ (μb)	$\sigma(14\,\text{TeV})$ (μb)
4.5	1	1	2.38	218	341	520
4.75	1	1	1.82	185	291	446
5	1	1	1.40	158	250	386
4.75	0.5	0.5	2.72	209	316	466
4.75	1	0.5	2.67	273	432	665
4.75	0.5	1	1.87	130	196	287
4.75	2	2	1.25	168	271	426
4.75	1	2	1.33	134	211	323
4.75	2	1	1.74	220	354	553

Table 4: Bottom total cross sections obtained from the parameter sets used to determined the theoretical uncertainty band in pp collisions with the CTEQ6M densities.

Obtaining the Electron Spectra From Heavy Flavor Decays

D and B decays to leptons depends on measured decay spectra and branching ratios

$D \to e$ Use preliminary CLEO data on inclusive electrons from semi-leptonic D decays, assume it to be indentical for all charm hadrons

$B \to e$ Primary B decays to electrons measured by Babar and CLEO, fit data and assume fit to work for all bottom hadrons

$B \to D \to e$ Obtain electron spectrum from convolution of $D \to e$ spectrum with parton model calculation of $b \to c$ decay

Branching ratios are admixtures of charm and bottom hadrons

$$\begin{aligned} B(D \to e) &= 10.3 \pm 1.2\,\% \\ B(B \to e) &= 10.86 \pm 0.35\,\% \\ B(B \to D \to e) &= 9.6 \pm 0.6\,\% \end{aligned}$$

Uncertainty Bands for Electrons from Heavy Flavor Decays at 200 GeV

Electrons from B decays begin to dominate at $p_T \sim 5$ GeV

Electron spectra very sensitive to rapidity range – to get $|y| \leq 0.75$ electrons, need $|y| \leq 2$ charm and bottom range

Forward electron spectra thus not possible to obtain using FONLL code due to problems at large y

.

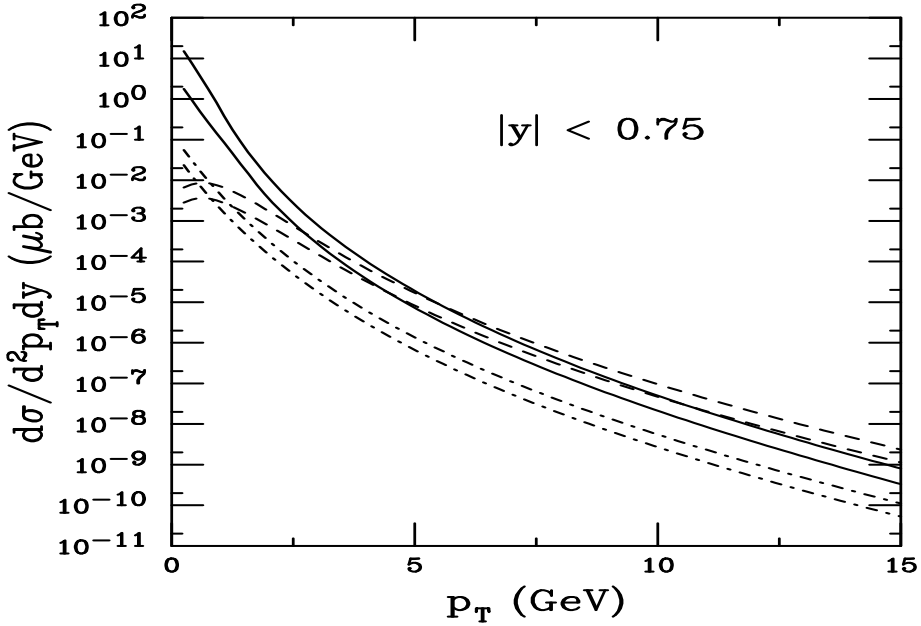

Figure 22: The theoretical FONLL bands for $D \to eX$ (solid), $B \to eX$ (dashed) and $B \to DX \to eX'$ (dot-dashed) as a function of p_T in $\sqrt{s} = 200$ GeV pp collisions for $|y| < 0.75$.

Comparison to Electron Data at 200 GeV

Includes PHENIX preliminary data from *pp* and STAR published and preliminary data

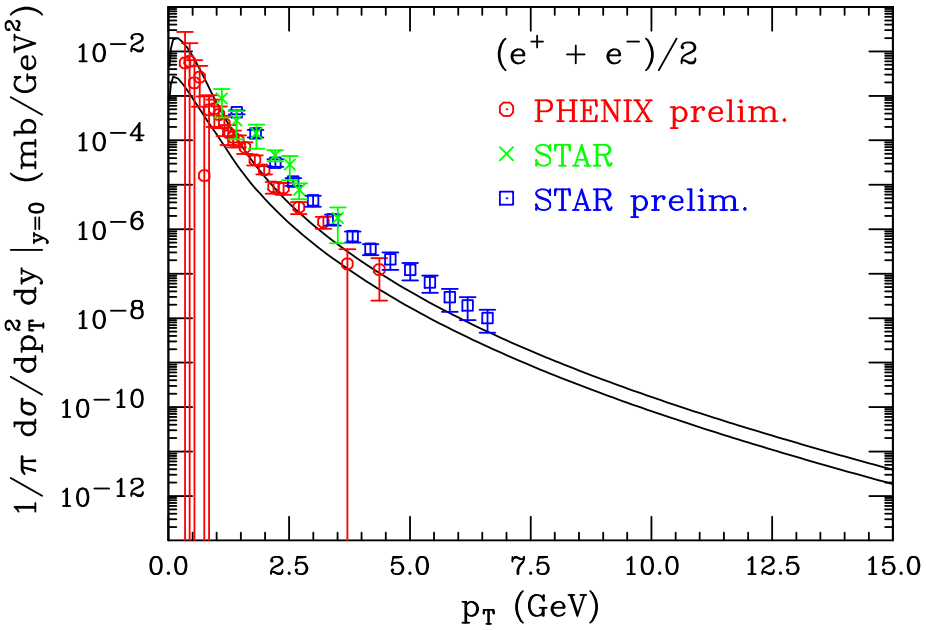

Figure 23: Prediction of the theoretical uncertainty band of the total electron spectrum from charm and bottom (Cacciari, Nason and RV). Preliminary data from PHENIX and STAR are also shown.

Uncertainty Bands for Electrons from Heavy Flavor Decays at 5.5 TeV

Crossover between B and D dominance harder to distinguish at LHC energy

Electron spectra much harder with increased energy

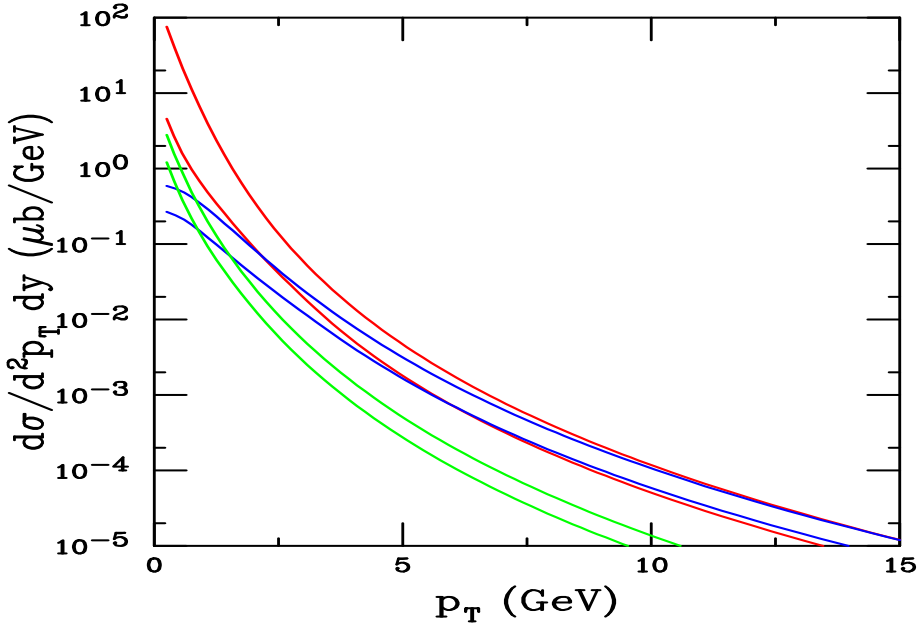

Figure 24: The theoretical bands for $D \to eX$ (red curves), $B \to eX$ (blue curves) and $B \to DX \to eX'$ (green curves) as a function of p_T in $\sqrt{s} = 5.5$ TeV pp collisions for $|y| < 1$.

Summary

- Theoretical uncertainty bands for charm must be constructed carefully due to low x and low μ behavior of parton densities
- This influences how well we can extrapolate to higher energies
- More modern fragmentation functions for D and B mesons indicate that the meson distribution is more similar to the quark distribution to higher p_T than previously assumed from older e^+e^- fits
- Contributions of D and B decays to leptons more difficult to disentangle at LHC and would require precision measurements of their decays to hadrons to better distinguish
- Variety of decay channels needed to sort out results